Environmental Pollution 221 (2017) 470–479

Contents lists available at ScienceDirect

Environmental Pollution

journal homepage: www.elsevier.com/locate/envpol

Co-transport of chlordecone and sulfadiazine in the presence of functionalized multi-walled carbon nanotubes in soils☆

Miaoyue Zhang [a, e, *], Irina Engelhardt [a, b], Jirka Šimůnek [c], Scott A. Bradford [d], Daniela Kasel [a], Anne E. Berns [a], Harry Vereecken [a], Erwin Klumpp [a]

[a] Agrosphere Institute (IBG-3), Forschungszentrum Jülich GmbH, 52425 Jülich, Germany
[b] TU Freiberg, Department of Hydrogeology, 09596 Freiberg, Germany
[c] Department of Environmental Sciences, University of California Riverside, Riverside, CA 92521, USA
[d] United States Department of Agriculture, Agricultural Research Service, U. S. Salinity Laboratory, Riverside, CA 92507, USA
[e] Institute for Environmental Research (Biology V), RWTH Aachen University, Worringerweg 1, 52074 Aachen, Germany

ARTICLE INFO

Article history:
Received 22 June 2016
Received in revised form
6 November 2016
Accepted 12 December 2016
Available online 21 December 2016

Keywords:
Colloid-facilitated contaminant transport
Multi-walled carbon nanotubes
Soil
Retention profile
Numerical modeling

ABSTRACT

Batch and saturated soil column experiments were conducted to investigate sorption and mobility of two ^{14}C-labeled contaminants, the hydrophobic chlordecone (CLD) and the sulfadiazine (SDZ), in the absence or presence of functionalized multi-walled carbon nanotubes (MWCNTs). The transport behaviors of CLD, SDZ, and MWCNTs were studied at environmentally relevant concentrations (0.1–10 mg L^{-1}) and they were applied in the column studies at different times. The breakthrough curves and retention profiles were simulated using a numerical model that accounted for the advective-dispersive transport of all compounds, attachment/detachment of MWCNTs, equilibrium and kinetic sorption of contaminants, and co-transport of contaminants with MWCNTs. The experimental results indicated that the presence of mobile MWCNTs facilitated remobilization of previously deposited CLD and its co-transport into deeper soil layers, while retained MWCNTs enhanced SDZ deposition in the topsoil layers due to the increased adsorption capacity of the soil. The modeling results then demonstrated that the mobility of engineered nanoparticles (ENPs) in the environment and the high affinity and entrapment of contaminants to ENPs were the main reasons for ENP-facilitated contaminant transport. On the other hand, immobile MWCNTs had a less significant impact on the contaminant transport, even though they were still able to enhance the adsorption capacity of the soil.

1. Introduction

Multi-walled carbon nanotubes (MWCNTs) consist of multiple rolled layers (concentric tubes) of graphene (Iijima, 1991; Kasel et al., 2013a). Due to their unique physical and chemical properties, carbon nanotubes (CNTs) have been used in various applications (Gannon et al., 2007; Gohardani et al., 2014; Mattison et al., 2011), which will undoubtedly result in their release into the environment. Recent studies have additionally reported that various organic or inorganic contaminants such as pesticides, antibiotics, and heavy metals can sorb to and be transported by CNTs (Jośko et al., 2013; Kim et al., 2014; Luo et al., 2013; Ren et al., 2011). An important implication of the CNTs presence in the environment is that they may significantly affect the fate of various contaminants and that they may potentially be used for their remediation.

To date, only a few studies have investigated the transport behavior of CNTs in natural soils or in model soil systems. These studies have reported that the transport behavior of CNTs is affected by ionic strength, flow velocity, structure of porous media, their input concentrations, and their structure/shape (Jaisi et al., 2008; Kasel et al., 2013a; Mattison et al., 2011; Tian et al., 2012; Wang et al., 2012). Kasel et al. (2013b) found only limited transport of functionalized MWCNTs in undisturbed and unsaturated soils. Fang et al. (2013) showed that the mobility of CNTs suspended in a nonionic surfactant solution varied with the size of soil particles and the soil's sand content, and was negatively correlated to the soil's clay content. However, current knowledge about the fate and transport of CNTs in soils is still rather limited. There are even fewer studies on the effects of CNTs on the mobility of other solutes

☆ This paper has been recommended for acceptance by Baoshan Xing.
* Corresponding author.
E-mail address: m.zhang@fz-juelich.de (M. Zhang).

http://dx.doi.org/10.1016/j.envpol.2016.12.018
0269-7491/

and compounds, such as organic and inorganic contaminants, in soils.

In general, colloids (e.g., suspended nanoparticles, clay particles, and metal oxides) in the subsurface can act as carriers for contaminants because of their mobility and large sorption capacity. This process is often defined as "colloid-facilitated contaminant transport" (co-transport) (Bradford and Kim, 2010; Šimůnek et al., 2006, 2012). However, only very few studies have investigated the co-transport between engineered nanoparticles (ENPs) and contaminants (Hofmann and Von der Kammer, 2009; Su et al., 2016; Zhang et al., 2011). These studies reported that ENPs affect the contaminant transport if nanoparticles have a strong mobility in porous media, a high adsorption capability, or if they are present in high concentrations (Hofmann and Von der Kammer, 2009; Zhang et al., 2011). These studies used a mixture of ENPs and contaminants. However, it is relatively unlikely that ENPs and contaminants are simultaneously released into the environment. To the best of our knowledge, there have been no soil columns experimental and numerical analysis concerning the fate and transport of CNTs and contaminants that were not released simultaneously. Such studies could simulate a possible soil remediation scenario when CNTs are released, either on purpose or accidentally, into an initially contaminated soil.

Numerical models simulating colloid-facilitated contaminant transport are generally based on the mass balance equations for both colloids and contaminants and account for various interactions between the colloids, contaminants, and soil. They consider various equilibrium and kinetic models such as the first-order sorption of contaminants to soil, the first-order kinetic attachment of colloids (Jin et al., 1997; Treumann et al., 2014), irreversible nonlinear kinetic attachment of colloids (Bradford et al., 2011), and competitive Langmuir kinetic sorption of contaminants on colloids (van de Weerd and Leijnse, 1997). In this study, additional processes are considered in the numerical analysis of the experimental data, including blocking and depth-dependent retention of MWCNTs during transport (Kasel et al., 2013a) and a non-simultaneous release of MWCNTs and contaminants (Pang and Šimůnek, 2006; Šimůnek et al., 2006).

The aim of this study is to investigate the sorption and mobility of two different contaminants chlordecone (CLD, $C_{10}Cl_{10}O$), a highly chlorinated pesticide, and sulfadiazine (SDZ, 4-amino-*N*-pyrimidin-2-yl-benzenesulfonamide), a widely used sulfonamide antibiotics, in the absence and presence of functionalized MWCNTs. CLD is a persistent organic pollutant that remains present in soils almost 20 years after its prohibition due to its long-term application (Cabidoche and Lesueur-Jannoyer, 2012; Fernandez-Bayo et al., 2013b). The intense usage of antibiotics such as SDZ led to their wide distribution in the environment (McArdell et al., 2003; Pailler et al., 2009; Tamtam et al., 2008). In this study, the transport behavior of MWCNTs in combination with the contaminants SDZ and CLD is investigated by analyzing adsorption isotherms, as well as breakthrough curves and retention profiles of column experiments. The column data are analyzed using the C-Ride module (Šimůnek et al., 2012) of HYDRUS-1D (Šimůnek et al., 2016), which accounts for advective-dispersive transport of both colloids and contaminants, attachment, detachment and straining of colloids, and kinetic sorption of contaminants to both soil and colloids.

2. Materials and methods

2.1. Chemicals

Radioactively (^{14}C) labeled and unlabeled MWCNTs were applied for the batch and column experiments (Bayer Technology Services GmbH, 51368 Leverkusen, Germany). MWCNTs were boiled with 70% nitric acid (Sigma-Aldrich Chemie GmbH, 89555 Steinheim, Germany) for 4 h, resulting in additional oxygen-containing functional groups (e.g., carboxylic groups) on their surfaces. Kasel et al. (2013a, 2013b) found limited transport of MWCNT in soil and (small grain size) quartz sand even under unfavorable attachment conditions (negative charge of both MWCNTs and porous media at low ionic strength) and suggested that this was due to particle straining and aggregation, implying that the colloidal stability of the MWCNT suspension was a significant factor. Therefore, the MWCNT suspensions were prepared with 1 mM KCl and ultrasonicated for 15 min at 65 W by a cup horn sonicator as stock suspension, and then ultrasonicated again for 10 min before injection, leading to better-dispersed MWCNTs during the experiments. This MWCNTs suspension (1 mg L^{-1}, 1 mM KCl) was found to be stable for at least 24 h after preparation (Kasel et al., 2013a). The characterization and aggregation behavior of functionalized MWCNTs is given in Kasel et al. (2013a, 2013b).

Radioactively (^{14}C) labeled CLD dissolved in acetone was purchased from Moravek Biochemicals (Brea, CA, USA). The specific radioactivity of ^{14}C-labeled CLD was 2.94 MBq mg^{-1}. For preparation of the desired CLD solution concentration, non-labeled CLD (Sigma-Aldrich Chemie GmbH, Steinheim, Germany) was mixed with the ^{14}C-labeled CLD. The total mass of non-labeled CLD and ^{14}C-labeled CLD was approximately 1 mg. After the acetone had evaporated, the flasks were filled with 1 L of 1 mM KCl.

Radioactively (^{14}C) pyrimidine-ring-labeled SDZ was purchased from Bayer-Health Care AG (Wuppertal, Germany) and dissolved in the 1 mM KCl solution for the desired concentration. The specific radioactivity was 0.43 MBq mg^{-1}. All ^{14}C-labeled samples were added to 5 ml of scintillation cocktail (Insta-Gel Plus, Perkin Elmer, USA) and measured using a liquid scintillation counter (LSC, Perkin Elmer, USA).

2.2. Batch experiments

In accordance with OECD guideline 106 (OECD., 2000), the adsorption kinetics and the adsorption isotherms of CLD on the loamy sand soil and on MWCNTs were determined in batch trials and by using the dialysis technique (Höllrigl-Rosta et al., 2003), respectively. The soil adsorption isotherms were measured using mixtures of 10 ml ^{14}C-labeled CLD solutions of different concentrations and 1 g soil (in 1 mM KCl), which were equilibrated for 24 h in an overhead shaker. After centrifugation, the supernatant was taken and measured by LSC. The dialysis technique (Höllrigl-Rosta et al., 2003) was applied to determine the adsorption of CLD and SDZ on MWCNTs. Two dialysis half-cells were therefore separated by a 1 kDa cut-off cellulose membrane and inserted into a special frame. Then, the bottom part of the half-cell was filled with approximately 5 ml of MWCNT suspension (non-labeled, 10 mg L^{-1}) and the top part of the half-cell was filled with 5 ml of CLD (0–10 μg g^{-1}) or SDZ (0–1 mg L^{-1}) at selected concentrations. The filled half-cell was then rotated at 10 rpm for 48 h. After equilibration, the solution concentration of ^{14}C-labeled CLD or SDZ in the top part of the half-cell was measured by LSC.

The sorption kinetics of CLD to MWCNTs were determined by adding 10 ml of 10 μg g^{-1} of ^{14}C-labeled CLD solution to 10 mg of unlabeled MWCNTs, and then mixing. This suspension was centrifuged at selected time intervals and a sample of the supernatant was measured by LSC. The kinetic analysis of the batch experimental data was carried out using the following equation (Schijven and Hassanizadeh, 2000):

$$\frac{C}{C_0} = \frac{k_{dmM} + k_{amM}\exp[-(k_{amM} + k_{dmM})t]}{k_{amM} + k_{dmM}} \quad (1)$$

where C is the contaminant concentration in the liquid phase [ML^{-3}]; C_0 is the initial contaminant concentration in the liquid phase [ML^{-3}]; k_{amM} and k_{dmM} are the CLD adsorption and desorption rate coefficients to the mobile MWCNTs [T^{-1}], respectively. The calculated adsorption and desorption rate coefficients (k_{amM} and k_{dmM}) are given in Table 1. Blank experiments were conducted to determine the sorption of CLD, SDZ, and MWCNTs to wall of the centrifuge tubes or the dialysis membrane in the batch experiments. Batch concentrations in the presence of soil or MWCNTs were corrected for sorption losses in blank experiments.

2.3. Transport experiments

Stainless steel columns (3 cm inner diameter and 12 cm length) were used for transport experiments. Samples of the loamy sand soil were taken from the upper 30 cm in Kaldenkirchen-Hülst, Germany (sieved to a fraction < 2 mm and air dried, and the median grain size, d_{50}, equaled 120 μm). This soil had a total organic carbon of 1.1% mass, a cationic exchange capacity of 7.8 $cmol_c\ kg^{-1}$, and pH value of 5.9 (Kasel et al., 2013b). The soil was composed of 4.9% clay (<2 μm), 26.7% silt (2–63 μm), and 68.5% sand (>2 μm). Soil and deionized water were alternately and incrementally filled into the columns. The columns were then connected to a pump (MCP V 5.10, Ismatec SA, Glattbrugg, Switzerland), with the flow direction from the bottom to the top of the column. Approximately 30 pore volumes (PVs) of background electrolyte solution (1 mM KCl) were applied to the column before the transport experiments were carried out. The bulk density of the packed columns was approximately 1.48 g cm^{-3}.

A tracer experiment was conducted first to characterize the hydraulic conditions and conservative transport parameters, such as porosity and dispersivity, of the soil. A pulse of approximately 2.1 PV (about 90 mL) of the tracer (1 mM KBr) was applied for that purpose. Effluent solutions were collected by a fraction collector every 30 s (e.g., approximately 2.5 mL per vial) and analyzed to determine the breakthrough curves (BTCs). The effluent concentrations of bromide were determined using a high-performance liquid chromatograph (STH 585, Dionex, Sunnyvale, CA, USA) equipped with a UV detector (UV2075, Jasco, Essex, UK).

The same procedure was repeated when CLD, SDZ, and MWCNTs were applied. The single-species transport of CLD (^{14}C-labeled, experiment I), SDZ (^{14}C-labeled, experiment II and III), or MWCNTs (^{14}C-labeled, experiment IV) in the saturated soil columns were investigated first. Based on information collected during this first step, the second set of column experiments was designed to investigate the effect of MWCNTs on the transport of CLD and SDZ. During the CLD co-transport experiment, a pulse (around 2.1 PV) of CLD (^{14}C-labeled) was injected first, followed by a MWCNT suspension pulse (non-labeled, around 2.1 PV) applied at the same ionic strength and flow velocity (experiment V and VI). In contrast, during the SDZ co-transport experiment, the MWCNT suspension (non-labeled, around 2.1 PV) was injected first, followed by an injection of SDZ (^{14}C-labeled, around 2.1 PV, experiments VII and VIII). For both CLD and SDZ co-transport experiments, the non-^{14}C-labeled MWCNTs, prepared in the same way as the ^{14}C-labeled MWCNTs, were applied. We assumed that the non-labeled MWCNTs in the co-transport experiments showed the same transport behavior as the ^{14}C-labeled MWCNTs in the single-species transport experiments. A summary of the experimental conditions is provided in Table 2. The retardation factor (R) can be calculated from the mean breakthrough time (t_b), the column length (L), and the pore-water velocity (v) as $R=t_bv/L$. The value of R is a measure of the mean breakthrough time relative to a conservative solute tracer.

At the end of the experiments, soil samples were excavated from the columns in approximately 0.5–1 cm thick increments and analyzed to determine the retention profiles (RPs) of CLD, SDZ, and MWCNTs. The soil samples of each layer were dried, crushed and combusted using a biological oxidizer at 900 °C (OX 500, R.J. Harvey Instrumentation Corporation, Tappan, NY, USA), followed by the LSC measurement. Before the column experiments, empty columns without soil were used to determine losses of MWCNTs, CLD, and SDZ to ensure the appropriateness of the column setup. The loss percentage to the empty column was approximately 3%.

Table 1
Optimized results from batch experiments.

Chemicals	Absorbents	k_{amM} [min^{-1}]	k_{dmM} [min^{-1}]	K_d [cm^3g^{-1}]	K_{oc} [cm^3g^{-1}]
CLD	MWCNT	0.10	5.32E-03	60,000	NF
CLD	soil			56	5090
SDZ	MWCNT			6000	NF
SDZ[a]	soil			0.56	5.09

NF - not fitted.
[a] The adsorption of SDZ in the soil was described by Zarfl (2008).

2.4. Numerical modeling

The C-Ride module (Šimůnek et al., 2012) of HYDRUS-1D (Šimůnek et al., 2016) was used to simulate the one-dimensional transport and co-transport of CLD, SDZ, and MWCNTs. The transport of MWCNTs can be described using the advection-dispersion equation coupled with one-site kinetic retention as follows (Bradford et al., 2003; Gargiulo et al., 2007):

$$\theta\frac{\partial C_M}{\partial t} + \rho\frac{\partial S_M}{\partial t} = \theta D_M\frac{\partial^2 C_M}{\partial x^2} - q\frac{\partial C_M}{\partial x} \quad (2)$$

$$\rho\frac{\partial S_M}{\partial t} = \theta\psi k_{ac}C_M - \rho k_{dc}S_M \quad (3)$$

where θ is the volumetric water content [L^3L^{-3}], C_M is the MWCNT concentration in the liquid phase [nL^{-3}], t is time [T], ρ is the bulk density of the soil [ML^{-3}], S_M is the MWCNT concentration associated with (attached or strained) the soil [nM^{-1}], x is the spatial coordinate [L], D_M is the hydrodynamic dispersion coefficient for MWCNTs [L^2T^{-1}], q is the Darcy velocity [LT^{-1}], k_{ac} and k_{dc} are the first-order attachment and detachment coefficients for MWCNTs [T^{-1}], respectively, and ψ [-] is the dimensionless MWCNT retention function to account for time- and depth-dependent retention, which is defined as:

$$\psi = \left(1 - \frac{S_M}{S_M^{max}}\right)\left(\frac{d_{50} + x}{d_{50}}\right)^{-\beta} \quad (4)$$

where d_{50} is the median grain size of the soil [L], β [-] is a parameter which is controlled by the shape of the retention profile, S_M^{max} is the maximum solid phase MWCNT concentration [nM^{-1}]. In this study, a β value of 0.765 was employed for non-spherical MWCNTs (Kasel et al., 2013a, 2013b).

Contaminant (CLD or SDZ) transport in soil was described using the advection-dispersion equation:

Table 2
Experimental conditions, hydraulic parameters and mass balance information for all column experiments. The ionic strength for all column experiments was 1 mM KCl and d_{50} of soil was 120 μm.

Single-species transport experiments								
Chemical	No.	C_o [mg L^{-1}]	q [cm min^{-1}]	Porosity	λ [cm]	M_{eff}	M_{soil}	M_{total}
CLD	I	1	0.71	0.5	0.16	0.007	1.002	1.009
SDZ	II	0.1	0.70	0.52	0.18	0.937	0.118	1.056
SDZ	III	1	0.72	0.49	0.31	0.981	0.030	1.011
MWCNTs	IV	1	0.72	0.50	0.60	0.458	0.488	0.946

Co-transport experiments									
Chemical	No.	C_o [mg L^{-1}]		q [cm min^{-1}]	Porosity	λ [cm]	M_{eff}	M_{soil}	M_{total}
		MWCNTs	CLD/SDZ						
CLD/MWCNTs	V	1	1	0.71	0.51	0.16	0.010	1.008	1.017
CLD/MWCNTs	VI	10	1	0.71	0.54	*NF*	0.010	0.997	1.007
MWCNTs/SDZ	VII	1	1	0.70	0.50	0.09	0.976	0.073	1.049
MWCNTs/SDZ	VIII	1	0.1	0.69	0.52	0.21	0.884	0.280	1.164

Co is the input concentration; λ is the hydrodynamic longitudinal dispersivity estimated from Br; M_{eff} is the fraction of MWCNT, CLD, or SDZ mass in the effluent; M_{soil} is the fraction of MWCNT, CLD, or SDZ mass in the solid phase; M_{total} is the total relative mass for the column experiment; NF - not fitted.

$$\theta\frac{\partial C}{\partial t}+\rho\frac{\partial S}{\partial t}=\theta D\frac{\partial^2 C}{\partial x^2}-q\frac{\partial C}{\partial x} \tag{5}$$

where C is the contaminant concentration in the liquid phase [ML^{-3}], D is the hydrodynamic dispersion coefficient for CLD or SDZ [L^2T^{-1}], S is the contaminant concentration sorbed to the solid phase [MM^{-1}]. Sorption of CLD or SDZ was described using a two-site adsorption-desorption model as follows (Van Genuchten and Wagenet, 1989):

$$S=S_e+S_k \tag{6}$$

$$\frac{\partial S_e}{\partial t}=fK_d\frac{\partial C}{\partial t} \tag{7}$$

$$\frac{\partial S_k}{\partial t}=\omega[(1-f)K_dC-S_k] \tag{8}$$

where S_e [MM^{-1}] is the contaminant concentration on instantaneous equilibrium sorption site, S_k [MM^{-1}] is the contaminant concentration on the remaining first-order kinetic sorption site, f [-] is the fraction of exchange sites assumed to be in equilibrium with the solution phase, K_d is the partition coefficient for linear adsorption [L^3M^{-1}], ω is the first-order rate constant [T^{-1}]. The diffusion coefficients of CLD and SDZ are from Pritchard et al. (1986) and Chen et al. (2013), respectively. Due to the short duration of the experiments, degradation and transformation of contaminants can be neglected.

The interactions between the contaminant (CLD or SDZ) and mobile or immobile MWCNTs during coupled nanotubes and contaminant transport are described as follows (Pang and Šimůnek, 2006; Šimůnek et al., 2006, 2012):

$$\theta\frac{\partial C}{\partial t}+\rho\frac{\partial S_e}{\partial t}+\rho\frac{\partial S_k}{\partial t}+\theta\frac{\partial C_MS_{mM}}{\partial t}+\rho\frac{\partial S_MS_{iM}}{\partial t}=\theta D\frac{\partial^2 C}{\partial x^2}-q\frac{\partial C}{\partial x}++\theta D\frac{\partial^2 C_MS_{mM}}{\partial x^2}-q\frac{\partial C_MS_{mM}}{\partial x} \tag{9}$$

where S_{mM} and S_{iM} [MM^{-1}] are the CLD or SDZ concentrations sorbed to mobile and immobile MWCNTs, respectively. Concentrations of CLD or SDZ sorbed to immobile and mobile colloids can be written as follows:

$$\theta\frac{\partial C_MS_{mM}}{\partial t}=\theta D\frac{\partial^2 S_{mM}C_M}{\partial x^2}-q\frac{\partial C_MS_{mM}}{\partial x}+\theta\psi_mk_{amM}C-\theta k_{dmM}C_MS_{mM}-\theta k_{ac}C_MS_{mM}+\rho k_{dc}S_MS_{iM} \tag{10}$$

$$\rho\frac{\partial S_MS_{iM}}{\partial t}=\theta\psi_{im}k_{aiM}C-\rho k_{diM}S_MS_{iM}+\theta k_{ac}C_MS_{mM}-\rho k_{dc}S_MS_{iM} \tag{11}$$

where k_{aiM} and k_{diM} are the rate coefficients for CLD or SDZ sorption to and desorption from immobile MWCNTs [T^{-1}], respectively; and ψ_m and ψ_{im} are dimensionless variables that adjust the sorption rate to a number of mobile and immobile MWCNTs present, respectively. Detailed list of all transport and reaction equations involved in colloid-facilitated solute transport are described in detail in the manual of C-Ride.

3. Results and discussion

3.1. Adsorption of CLD and SDZ on MWCNTs and soil

All the optimized results from batch experiments are summarized in Table 1. A linear adsorption isotherm provided a good description of CLD adsorption on the soil ($r^2 = 0.99$, Table 1, Fig. 1a). The sorption coefficient (K_d) equaled 56 $cm^3\ g^{-1}$. This value of K_d can be used in conjunction with the soil organic carbon fraction (f_{oc} = 0.011 g g^{-1}) (Kasel et al., 2013b) to calculate the organic carbon normalized adsorption coefficient ($K_{oc} = K_d/f_{oc}$) (OECD., 2000) that is equal to $cm^3\ g^{-1}$. This K_{oc} value is consistent with the reported range in the literature of 2500 to 20,000 $cm^3\ g^{-1}$ (Woignier et al., 2012) and indicates that CLD sorption on the soil is mainly controlled by hydrophobic interactions with soil organic carbon (Cabidoche et al., 2009; Levillain et al., 2012; Li et al., 2012), while inorganic soil components like clay minerals play a relatively minor role, which produces a limited mobility of CLD in soils (Fernandez-Bayo et al., 2013a; 2013b). The sorption of SDZ in the same (Kaldenkirchen-Hülst) soil was described in an earlier study (Zarfl, 2008). Reported values of K_d = 0.56 $cm^3\ g^{-1}$ and K_{oc} = 5.09 $cm^3\ g^{-1}$ indicate that organic carbon and inorganic soil components may both play an important role for SDZ sorption on the soil (Kasteel et al., 2010). However, SDZ has a much lower K_{oc} value than CLD, its mobility in soils is therefore expected to be

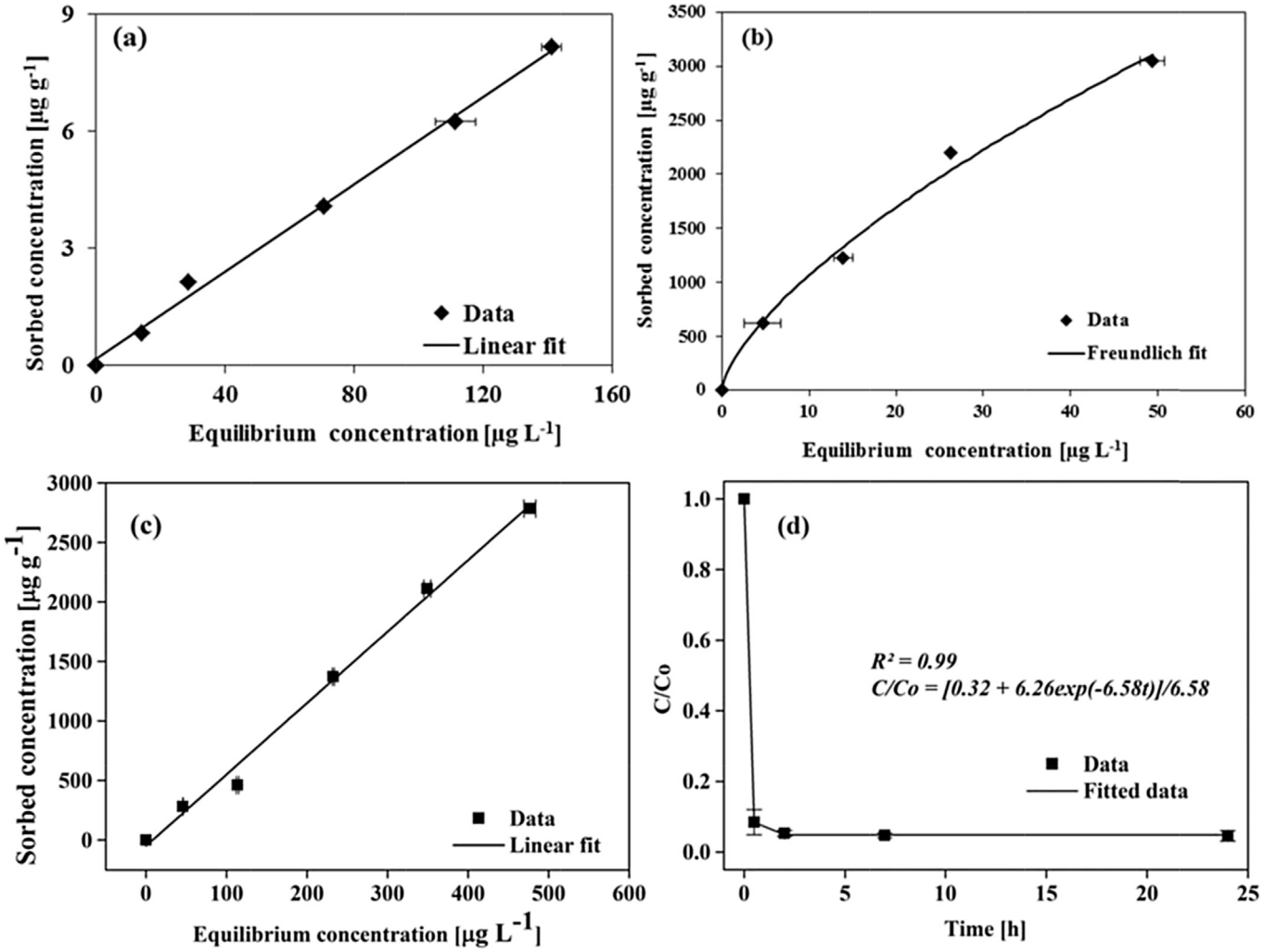

Fig. 1. (a) Adsorption isotherm of CLD on soil. (b) Adsorption isotherm of CLD on MWCNTs. (c) Adsorption isotherm of SDZ on MWCNTs. (d) Kinetic sorption data for CLD on MWCNTs.

Table 3
Parameters optimized by using different models for the CLD, SDZ, and MWCNT transport, co-transport and retention in soil.

Single-species transport experiments							
Experiment No.	r^2	MWCNT parameters			Contaminant (CLD or SDZ) parameters		
		S_M^{max}/C_0 [cm^3g^{-1}]	k_{ac} [min^{-1}]	k_{dc} [min^{-1}]	*Frac. (f)*	K_d [cm^3g^{-1}]	ω [min^{-1}]
I	0.827				5.46E-04	282.60	8.28E-04
II	0.963				0	0.17	1.22E-02
III	0.997				0	0.17	2.42
IV	0.975	5.45	10.3	6.80E-03			
Co-transport experiments							
Experiment No.		r^2			Contaminant (CLD or SDZ) parameters		
					k_{aiM} [min^{-1}]		k_{diM} [min^{-1}]
V		0.872			0.10[a]		5.32E-03[a]
VII		0.982			1.31E-02		1.02E-02
VIII		0.982			0.38		0.49

r correlation of observed and fitted data.
[a] - obtained from the batch experiments.

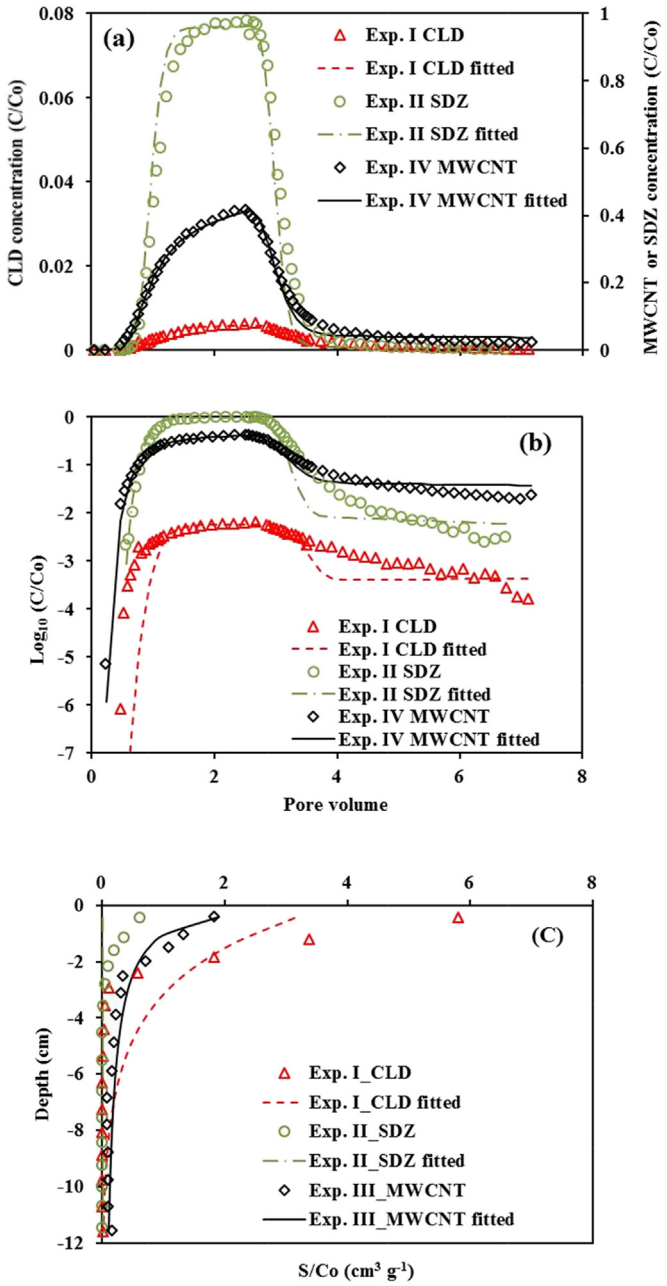

Fig. 2. Observed and estimated BTCs (a and b) and RPs (c) for a single-species transport of CLD (experiment I), SDZ (experiment II), and MWCNTs (experiment IV) in saturated soil columns. Figure (2a) has two vertical axes. The left axis shows the relative CLD concentrations (C/C_0), while the right axis shows the relative SDZ and MWCNTs concentrations. The breakthrough curves in Fig. b are plotted as log scale effluent concentrations ($\log_{10}C/Co$) versus pore volumes.

much higher than that of CLD.

The Freundlich equation provided a good description of adsorption isotherms of CLD on MWCNTs ($r^2 = 0.95$), with the Freundlich coefficient (K_F) and exponent (n) equal to 229 $\mu g^{(1-1/n)}$ $L^{1/n}$ g^{-1} and 1.49, respectively (Fig. 1b). The sorption coefficient K_d was calculated from a linear fit of the first part of the isotherm to be 60,000 cm^3 g^{-1}, which demonstrates strong adsorption. A linear adsorption isotherm provided a good description of SDZ adsorption on the MWCNTs ($r^2 = 0.99$, Fig. 1c), with a sorption coefficient K_d of 6000 cm^3 g^{-1}, which is in agreement with reported K_d values (10^3–10^4 cm^3g^{-1}) (Ji et al., 2009). The K_d values of CLD and SDZ on MWCNTs were three and five orders of magnitude higher than on the loamy sand soil, respectively. This strong adsorption capacity of large surface area MWCNTs for CLD and SDZ has been mainly been attributed to π-π dispersion and hydrogen-bonding interactions (Liao et al., 2008; Upadhyayula et al., 2009). The presence of MWCNTs in soils is therefore expected to strongly influence the mobility of CLD and SDZ.

Equation (1) provided a good description for the adsorption kinetics of CLD on MWCNTs ($r^2 = 0.99$, Fig. 1d). The adsorption (k_{amM}) and desorption (k_{dmM}) rate coefficients of CLD to/from the MWCNTs were determined to be 6.26 h^{-1} and 0.32 h^{-1}, respectively. The adsorption rate was much faster than the desorption rate.

3.2. Single-species transport of CLD, SDZ, and MWCNTs in soil

The first three column experiments (I, II, and IV) were performed to improve our understanding of the single-species transport behavior of CLD, SDZ, and MWCNTs in soils. The experimental conditions are presented in Table 2 and optimized model parameters in Table 3. The BTCs (Fig. 2a) are plotted as normalized effluent concentrations (C/C_0) versus pore volumes, where C_0 is the influent concentration. Effluent concentrations for CLD, SDZ, and MWCNTs were plotted on a log scale ($\log_{10}$ C/Co) in Fig. 2b versus pore volumes. The RPs (Fig. 2c) are plotted as normalized solid phase concentrations (S/C_0) versus column depth. The total recovered mass from the effluent and retained in the column ranged from 0.95 to 1.05 for the three compounds. The retardation factors for CLD, SDZ, and MWCNTs that were calculated from respective BTCs relative to the conservative tracer transport (Ptak et al., 2004) indicated that CLD, SDZ, and MWCNTs reached the column outlet with only a slight retardation compared to the conservative tracer (data not shown). Thus, pore size exclusion was not observed (Bradford et al., 2003).

Mass balance information in Table 2 shows that about half of the injected MWCNTs were retained in the soil column (Fig. 2, Table 2). Equations (2)–(5) provided a good description of the BTC and RP ($r^2 = 0.975$). The fitted value of k_{ac} was considerably (several orders of magnitude) higher than the k_{dc} (Table 3), indicating only a slow rate of release. The BTC exhibited blocking behavior (a decreasing rate of retention with continued MWCNT injection). The fitted value of $S_{max}/C_o = 5.45$ cm^3 g^{-1} was used to account for this blocking process, and its low value indicates that only a small fraction of the solid surface area contributed to MWCNT retention (Bradford et al., 2009; Kasel et al., 2013a). This result is expected because the soil and functionalized MWCNTs exhibit a net negative charge under low ionic strength conditions that produces an energy barrier to attachment (Bradford et al. 2006, 2009). The RP shape was hyperexponential (e.g., a greater rate of retention near the column inlet than the outlet). A number of potential explanations for hyperexponential RPs have appeared in the literature, including: straining (Bradford et al. 2002, 2003), heterogeneity in colloid size and charge (Bolster et al., 1999; Tong and Johnson, 2007; Tufenkji and Elimelech, 2005), and system hydrodynamics (Bradford et al., 2009; Wang et al., 2011). The exact reason of the hyperexponential RP cannot be deduced from the experimental data, but other literature information for the retention of MWCNTs suggests that straining was the domain process under our experimental conditions (Jaisi et al., 2008; Kasel et al., 2013a; Wang et al., 2012).

CLD and SDZ exhibited very different mobilities in the soil. Almost 100% of the CLD was retained in the soil, mostly in the shallow layers (0–2 cm). On the other hand, SDZ easily passed through the column and, only 12% was retained in the soil (Table 2). These results are consistent with the batch experiments, which found that the K_d value was much larger for CLD (56 cm^3 g^{-1}) than

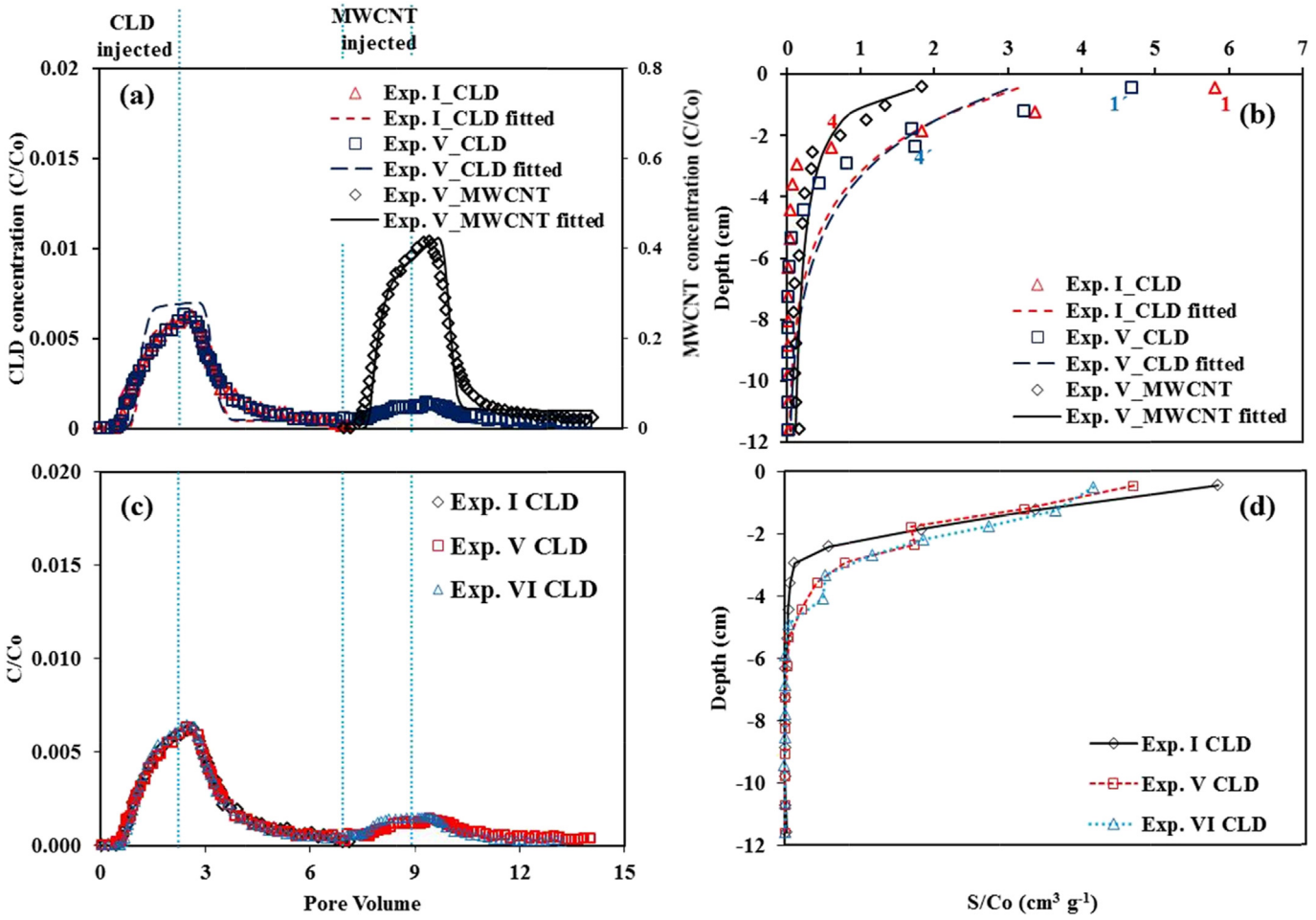

Fig. 3. Observed and estimated BTCs (a and c) and RPs (b and d) for CLD in single-species (experiment I) and co-transport (experiment V and VI, respectively) experiments in saturated soil columns. The input concentration for CLD and MWCNTs was 1 mg L^{-1}. Figure (3a) has two vertical axes. The left axis shows the relative CLD concentrations, while the right axis shows the relative MWCNT concentrations. The vertical dotted lines indicate applications of CLD and MWCNTs.

for SDZ (0.56 cm^3 g^{-1}). The two-site sorption model fitted well the observed BTCs for both CLD and SDZ (Table 3). Values of K_d that were fitted to the column experiments were not the same as those obtained in the batch experiments, especially for CLD. One plausible explanation is because continuous advection in the column systems produces kinetic sorption on the soil surface due to the shorter solute residence time than the equilibrium batch system. Indeed, the fitted fraction of equilibrium exchange sites (f) was always very small (Table 3), indicating that sorption of both CLD and SDZ was mainly a kinetic process. Equilibrium sorption can be neglected for SDZ due to the small value of K_d (0.17 cm^3 g^{-1}). Therefore, only a one-site kinetic sorption process was considered in the model by setting $f = 0$. In contrast, equilibrium sorption cannot be neglected for CLD because of the large value of K_d (282.6 cm^3 g^{-1}) that provides retardation of about 1.5. Unold et al. (2009) and Wehrhan et al. (2007) came to a similar conclusion for CLD and SDZ, even though they employed different sorption models. Fig. 2b demonstrates that low amounts of concentration tailing occurred following recovery of the breakthrough curves. Detachment/desorption was greatest for MWCNTs, SDZ, and then CLD.

Although the sorption model described experimental BTCs well, it was not able to correctly fit RPs with their hyper-exponential shapes (Fig. 2). The same problem was also encountered by Unold et al. (2009) and Wehrhan et al. (2007). The most plausible reason for the hyper-exponential RPs for CLD and SDZ is due to system hydrodynamics (Li et al., 2005). In particular, the same kinetic retention rate constant will produce greater amounts of CLD and SDZ removal in lower than higher velocity regions of the porous medium. The transport of CLD and SDZ is therefore expected to be controlled by high velocity regions with less removal with increasing distance.

3.3. Co-transport

Different injection sequences were employed in the co-transport experiments for CLD and SDZ in the presence of MWCNTs. Since CLD has a limited mobility in soil (Fig. 2), the CLD co-transport experiment was conducted by first injecting CLD into the soil column followed by a MWCNT suspension. This sequence was meant to simulate the process of using MWCNTs to remediate soil contaminated with CLD. On the other hand, MWCNTs retained in the soil influence the soil adsorption capacity and may thus affect the transport and sorption of highly mobile contaminants such as SDZ. The SDZ co-transport experiment was thus performed by injecting the MWCNT suspension first, followed by a SDZ pulse. This sequence was meant to simulate the process of using retained MWCNTs in the soil to slow down the spread of a contaminant, as is commonly done using reactive barriers.

The colloid-facilitated contaminant transport model in the C-

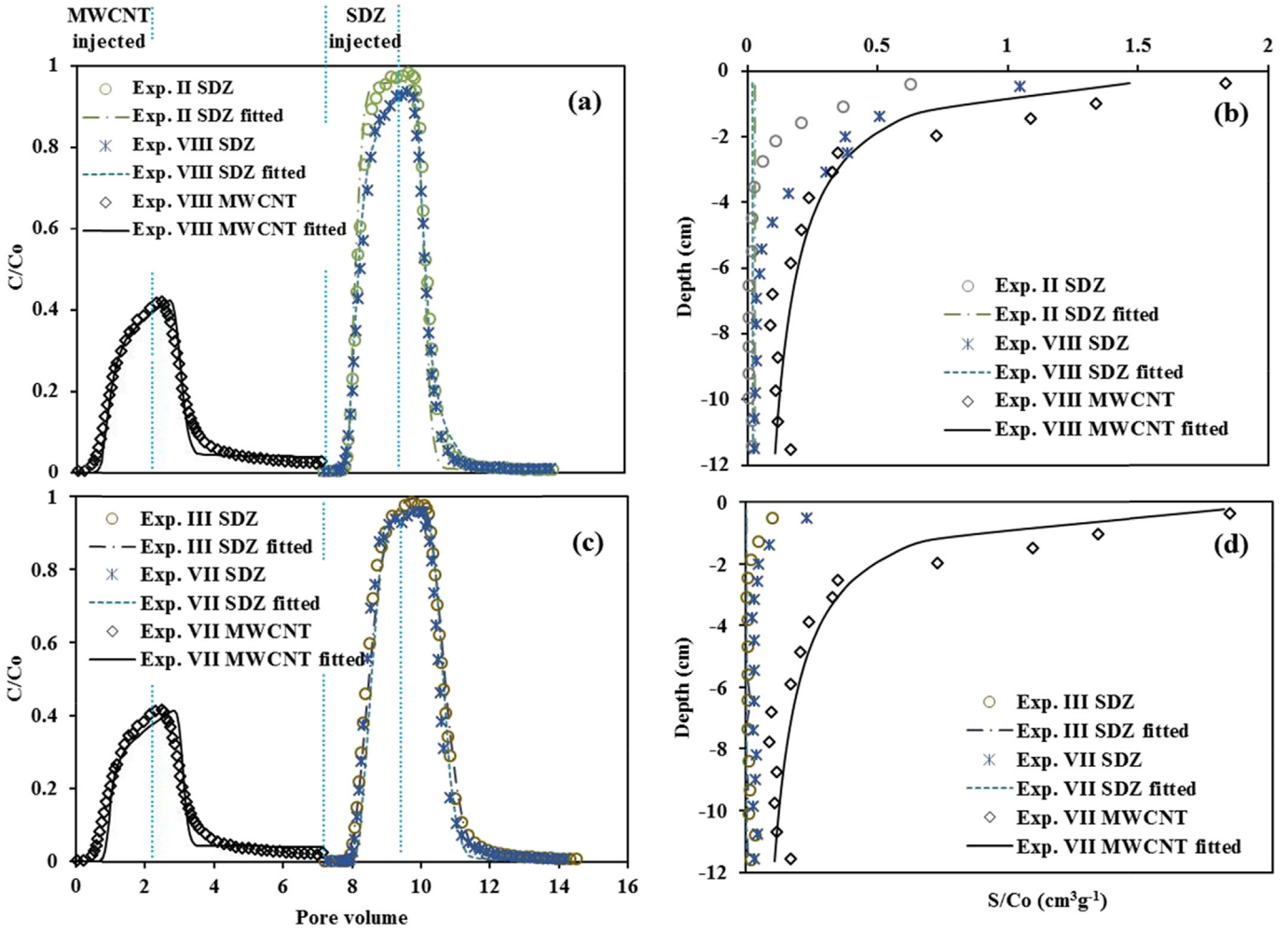

Fig. 4. Observed and estimated BTCs (a and c) and RPs (b and d) for single species SDZ (experiments II and III) and MWCNTs (experiment IV) or co-transport (experiment VII and VIII) experiments in saturated soil columns. The input concentration for SDZ and MWCNT was 0.1, 1 and 1 mg L^{-1}, respectively. The vertical dotted lines indicate applications of SDZ and MWCNTs.

Ride module of HYDRUS-1D was used to describe the interactions between CLD and SDZ with soil, and with mobile and retained MWCNTs in the four co-transport experiments (V, VI, VII and VIII, respectively). The interactions between CLD or SDZ (experiment I and II) and soil (ω, f, and K_d) were described using equations (5) through (8). The interactions between MWCNTs (experiment III) and soil (S_{max}, k_{ac} and k_{dc}) were described using equations (2) through (4). The interactions between CLD and mobile or retained MWCNTs were described by parameters k_{amM}, k_{dmM}, k_{aiM}, and k_{diM} using equations (9) through (11). The interactions between SDZ and retained MWCNTs were described by parameters k_{aiM} and k_{diM} using equations (9) through (11). As discussed above, rate parameters k_{amM} (6.26 h^{-1} = 0.10 min^{-1}) and k_{dmM} (0.32 h^{-1} = 5.32E-3 min^{-1}) were estimated from the sorption kinetic experiment (equation (1), Fig. 1d). We have assumed that adsorption or desorption rates of CLD to/from mobile and retained MWCNTs were the same and used these values ($k_{aiM} = k_{amM} = 0.10$ min^{-1} and $k_{diM} = k_{dmM} = 5.32E\text{-}3$ min^{-1}).

3.3.1. Pulse of CLD followed by pulse of MWCNTs

In experiments I, V and VI the effect of co-transport of CLD with MWCNTs under saturated conditions was investigated (Fig. 3). It is noteworthy that even though CLD's mobility is limited, it still appeared again in the outflow after the application of the MWCNTs suspension (Fig. 3a). The concentrations of retained CLD decreased approximately 11% in the first layer (point 1 and 1′, Fig. 3b) and increased nearly 8% in the fourth layer (point 4 and 4′, Fig. 3b) due to the MWCNT injection. Overall, nearly 17% of the CLD mass was remobilized from the top layers and shifted into deeper layers after injection of the MWCNT suspension (experiment I and V). This shift demonstrated that transport of MWCNTs facilitated the remobilization of CLD due to its strong sorption capacity for CLD. A similar trend was observed when CLD was injected prior to being eluted with a MWCNTs suspension at a higher input concentration of 10 mg L^{-1} (Fig. 3c and d).

Table 3 shows the optimized parameters of the CLD co-transport experiment. For both mobile and retained MWCNTs, the adsorption rate of CLD was much greater than desorption rate, which demonstrated that the sorption was a slowly reversible process and MWCNTs had a strong adsorption capacity for CLD.

3.3.2. Pulse of MWCNTs followed by pulse of SDZ

In experiments II, III, VII and VIII the influence of retained MWCNTs on SDZ transport and sorption was investigated (Fig. 4). While SDZ has a high mobility in soil, it was retained to a greater extent in soil in the presence of immobilized MWCNTs. About 12% of the SDZ was retained in the soil column when it was applied without MWCNTs (experiment II), whereas about 28% of the SDZ

was retained when it was applied after a MWCNT pulse (Fig. 4a and b, Table 2).

Mass balance information in Table 2 indicates that application of the MWCNT pulse reduced the SDZ mass that was recovered in the effluent (M_{eff}) by 5.3% and produced a corresponding increase in the SDZ mass that was retained in the soil (M_{soil}). These findings were further confirmed by conducting similar SDZ co-transport experiments (Fig. 4c and d, experiments III and VII) with a higher input concentration of SDZ ($C_0 = 1$ instead of 0.1 mg L^{-1}). Clearly, more SDZ was retained in the upper layer in the presence of MWCNTs when $C_0 = 1$ mg L^{-1} (Fig. 4c and d).

The isotherm data for SDZ on MWCNT (Fig. 1c) and soil (Table 1) suggest a linear increase in the retained SDZ concentration with C_0. Similarly, co-transport experiments conducted with a higher value of C_0 for SDZ also produced greater amounts of SDZ retention (Fig. 4). However, mass balance information in Table 2 indicates that the value of M_{soil} for SDZ was greater when the experiment was conducted with a lower (C_0 = 0.1 mg L^{-1}, experiment VIII) than higher ($C_0 = 1$ mg L^{-1}; experiment VII) input concentration of SDZ. Since the same amount of MWCNT (1 mg L^{-1}) was injected in both experiments, this implies that the relative amount of SDZ retention increased at a lower value of C_0 because the kinetic rate coefficients were much higher (Table 3). All these measures demonstrate that retained MWCNTs enhanced the sorption of SDZ in the soil column.

Unlike the CLD co-transport experiment that had both mobile and retained MWCNTs, SDZ only interacted with retained MWCNTs. Consequently, only parameters k_{aiM} and k_{diM} needed to be optimized to the SDZ co-transport experiments (Table 3). Fitted values of k_{aiM} were similar to k_{diM}, which demonstrated that SDZ sorption was a rapidly reversible process. In addition, estimated values of k_{aiM} and k_{diM} were strong functions of C_0 for SDZ, increasing with lower values of C_0. In particular, values of k_{aiM} and k_{diM} in experiment VIII (C_0 = 0.1 mg L^{-1} for SDZ) were about one order of magnitude higher than in experiment VII ($C_0 = 1$ mg L^{-1} for SDZ).

4. Conclusions

The hydrophobic pesticide CLD was found to have limited mobility in the soil because of its strong partitioning to the soil organic matter fraction. However, injection of MWCNTs facilitated the remobilization of a portion of the retained CLD from the soil because MWCNTs have a large sorption capacity for CLD and a greater mobility than CLD. These results demonstrate that mobile MWCNTs can facilitate the recovery of hydrophobic contaminants that are retained in soils. In contrast, the readily-water soluble antibiotic SDZ was found to be highly mobile in soil and exhibited small amounts of kinetic sorption to both soil organic and inorganic fractions. Immobilized MWCNTs in the soil diminished the transport of an injected pulse of SDZ because retained MWCNTs have a large sorption affinity for SDZ. Furthermore, the kinetic sorption rate for SDZ by MWCNTs was larger at lower SDZ concentrations, and this produced greater amounts of SDZ retention. Thus, immobilized MWCNTs can reduce the contaminant mass that migrates through the topsoil. Collectively, this research improves our understanding of how ENPs can enhance or diminish the transport of contaminants by considering: (i) non-simultaneous injection of ENPs and contaminants; (ii) environmentally relevant input concentrations for ENPs and contaminants; (iii) measurement of breakthrough curves and retention profiles for contaminants and ENPs; and (iv) numerical modeling of co-transport and interactions between ENPs and contaminants. It is worth noting that different environmental factors such as ionic strength, flow velocity, and soil types are known to have a large influence on MWCNT transport and retention. It is therefore expected that these same factors will have a large influence on co-transport scenarios with MWCNTs and contaminants, and additional research is needed to address these issues.

Acknowledgments

The first author thanks the China Scholarship Council for financial support. The authors would like to acknowledge Stephan Köppchen for his analysis of bromide in the liquid samples. The technical assistance of Herbert Philipp and Claudia Walraf is gratefully acknowledged. The present work was supported by the INRA Montpellier and the project CHLORDEXCO, funded by the French National Research Agency (ANR-08-CES-004-01), through the supply of the radioactive chlordecone. Thanks are also due to Dan Zhou for helping with the numerical investigations.

References

Bolster, C.H., Mills, A., Hornberger, G., Herman, J., 1999. Spatial distribution of deposited bacteria following miscible displacement experiments in intact cores. Water Res. Res. 35 (6), 1797–1807.
Bradford, S.A., Kim, H., 2010. Implications of cation exchange on clay release and colloid-facilitated transport in porous media. J. Environ. Qual. 39 (6), 2040.
Bradford, S.A., Kim, H.N., Haznedaroglu, B.Z., Torkzaban, S., Walker, S.L., 2009. Coupled factors influencing concentration-dependent colloid transport and retention in saturated porous media. Environ. Sci. Technol. 43 (18), 6996–7002.
Bradford, S.A., Šimůnek, J., Bettahar, M., Van Genuchten, M.T., Yates, S., 2006. Significance of straining in colloid deposition: evidence and implications. Water Res. Res. 42 (12).
Bradford, S.A., Šimůnek, J., Bettahar, M., van Genuchten, M.T., Yates, S.R., 2003. Modeling colloid attachment, straining, and exclusion in saturated porous media. Environ. Sci. Technol. 37 (10), 2242–2250.
Bradford, S.A., Torkzaban, S., Wiegmann, A., 2011. Pore-scale simulations to determine the applied hydrodynamic torque and colloid immobilization. Vadose Zone J. 10 (1), 252–261.
Bradford, S.A., Yates, S.R., Bettahar, M., Šimůnek, J., 2002. Physical factors affecting the transport and fate of colloids in saturated porous media. Water Res. Res. 38 (12), 63, 61–63–12.
Cabidoche, Y.M., Achard, R., Cattan, P., Clermont-Dauphin, C., Massat, F., Sansoulet, J., 2009. Long-term pollution by chlordecone of tropical volcanic soils in the French west Indies: a simple leaching model accounts for current residue. Environ. Pollut. 157 (5), 1697–1705.
Cabidoche, Y.M., Lesueur-Jannoyer, M., 2012. Contamination of harvested organs in root crops grown on chlordecone-polluted soils. Pedosphere 22 (4), 562–571.
Chen, C.-E., Zhang, H., Ying, G.-G., Jones, K.C., 2013. Evidence and recommendations to support the use of a novel passive water sampler to quantify antibiotics in wastewaters. Environ. Sci. Technol. 47 (23), 13587–13593.
Fang, J., Shan, X.-q., Wen, B., Huang, R.-x., 2013. Mobility of TX100 suspended multiwalled carbon nanotubes (MWCNTs) and the facilitated transport of phenanthrene in real soil columns. Geoderma 207–208, 1–7.
Fernandez-Bayo, J.D., Saison, C., Geniez, C., Voltz, M., Vereecken, H., Berns, A.E., 2013a. Sorption characteristics of chlordecone and cadusafos in tropical agricultural soils. Curr. Org. Chem. 17 (24), 2976–2984.
Fernandez-Bayo, J.D., Saison, C., Voltz, M., Disko, U., Hofmann, D., Berns, A.E., 2013b. Chlordecone fate and mineralisation in a tropical soil (andosol) microcosm under aerobic conditions. Sci. Total Environ. 463–464, 395–403.
Gannon, C.J., Cherukuri, P., Yakobson, B.I., Cognet, L., Kanzius, J.S., Kittrell, C., Weisman, R.B., Pasquali, M., Schmidt, H.K., Smalley, R.E., Curley, S.A., 2007. Carbon nanotube-enhanced thermal destruction of cancer cells in a noninvasive radiofrequency field. Cancer 110 (12), 2654–2665.
Gargiulo, G., Bradford, S., Šimůnek, J., Ustohal, P., Vereecken, H., Klumpp, E., 2007. Bacteria transport and deposition under unsaturated conditions: the role of the matrix grain size and the bacteria surface protein. J. Contam. Hydrology 92 (3–4), 255–273.
Gohardani, O., Elola, M.C., Elizetxea, C., 2014. Potential and prospective implementation of carbon nanotubes on next generation aircraft and space vehicles: a review of current and expected applications in aerospace sciences. Prog. Aerosp. Sci. 70, 42–68.
Hofmann, T., Von der Kammer, F., 2009. Estimating the relevance of engineered carbonaceous nanoparticle facilitated transport of hydrophobic organic contaminants in porous media. Environ. Pollut. 157 (4), 1117–1126.
Höllrigl-Rosta, A., Vinken, R., Lenz, M., Schäffer, A., 2003. Sorption and dialysis experiments to assess the binding of phenolic xenobiotics to dissolved organic matter in soil. Environ. Toxicol. Chem. 22 (4), 743–752.
Iijima, S., 1991. Helical microtubules of graphitic carbon. Nature 354 (6348), 56–58.
Jaisi, D.P., Saleh, N.B., Blake, R.E., Elimelech, M., 2008. Transport of single-walled carbon nanotubes in porous media: filtration mechanisms and reversibility. Environ. Sci. Technol. 42 (22), 8317–8323.
Ji, L., Chen, W., Zheng, S., Xu, Z., Zhu, D., 2009. Adsorption of sulfonamide antibiotics to multiwalled carbon nanotubes. Langmuir 25 (19), 11608–11613.
Jin, Y., Yates, M.V., Thompson, S.S., Jury, W.A., 1997. Sorption of viruses during flow

through saturated sand columns. Environ. Sci. Technol. 31 (2), 548–555.
Jośko, I., Oleszczuk, P., Pranagal, J., Lehmann, J., Xing, B., Cornelissen, G., 2013. Effect of biochars, activated carbon and multiwalled carbon nanotubes on phytotoxicity of sediment contaminated by inorganic and organic pollutants. Ecol. Eng. 60, 50–59.
Kasel, D., Bradford, S.A., Šimůnek, J., Heggen, M., Vereecken, H., Klumpp, E., 2013a. Transport and retention of multi-walled carbon nanotubes in saturated porous media: effects of input concentration and grain size. Water Res. 47 (2), 933–944.
Kasel, D., Bradford, S.A., Šimůnek, J., Pütz, T., Vereecken, H., Klumpp, E., 2013b. Limited transport of functionalized multi-walled carbon nanotubes in two natural soils. Environ. Pollut. 180 (0), 152–158.
Kasteel, R., Mboh, C.M., Unold, M., Groeneweg, J., Vanderborght, J., Vereecken, H., 2010. Transformation and sorption of the veterinary antibiotic sulfadiazine in two soils: a short-term batch study. Environ. Sci. Technol. 44 (12), 4651–4657.
Kim, H., Hwang, Y.S., Sharma, V.K., 2014. Adsorption of antibiotics and iopromide onto single-walled and multi-walled carbon nanotubes. Chem. Eng. J. 255, 23–27.
Levillain, J., Cattan, P., Colin, F., Voltz, M., Cabidoche, Y.-M., 2012. Analysis of environmental and farming factors of soil contamination by a persistent organic pollutant, chlordecone, in a banana production area of French West Indies. Agriculture. Ecosyst. Environ. 159 (0), 123–132.
Li, C., Ji, R., Schaffer, A., Sequaris, J.M., Amelung, W., Vereecken, H., Klumpp, E., 2012. Sorption of a branched nonylphenol and perfluorooctanoic acid on Yangtze river sediments and their model components. J. Environ. Monit. 14 (10), 2653–2658.
Li, X., Zhang, P., Lin, C., Johnson, W.P., 2005. Role of hydrodynamic drag on microsphere deposition and Re-Entrainment in porous media under unfavorable conditions. Environ. Sci. Technol. 39 (11), 4012–4020.
Liao, Q., Sun, J., Gao, L., 2008. The adsorption of resorcinol from water using multiwalled carbon nanotubes. Colloids Surfaces A Physicochem. Eng. Aspects 312 (2), 160–165.
Luo, C., Wei, R., Guo, D., Zhang, S., Yan, S., 2013. Adsorption behavior of Mno2 functionalized multi-walled carbon nanotubes for the removal of cadmium from aqueous solutions. Chem. Eng. J. 225, 406–415.
Mattison, N.T., O'Carroll, D.M., Kerry Rowe, R., Petersen, E.J., 2011. Impact of porous media grain size on the transport of multi-walled carbon nanotubes. Environ. Sci. Technol. 45 (22), 9765–9775.
McArdell, C.S., Molnar, E., Suter, M.J.-F., Giger, W., 2003. Occurrence and fate of macrolide antibiotics in wastewater treatment plants and in the glatt valley watershed, Switzerland. Environ. Sci. Technol. 37 (24), 5479–5486.
Test No. 106 OECD, 2000. Adsorption – Desorption Using a Batch Equilibrium Method.
Pailler, J.-Y., Krein, A., Pfister, L., Hoffmann, L., Guignard, C., 2009. Solid phase extraction coupled to liquid chromatography-tandem mass spectrometry analysis of sulfonamides, tetracyclines, analgesics and hormones in surface water and wastewater in Luxembourg. Sci. Total Environ. 407 (16), 4736–4743.
Pang, L., Šimůnek, J., 2006. Evaluation of bacteria-facilitated cadmium transport in gravel columns using the Hydrus colloid-facilitated solute transport model. Water Res. Res. 42 (12).
Pritchard, P.H., Monti, C.A., O'Neill, E.J., Ahearn, D.G., Connolly, J.P., 1986. Movement of Kepone®(chlordecone) across an undisturbed sediment-water interface in laboratory systems. Environ. Toxicol. Chem. 5 (7), 647–657.
Ptak, T., Piepenbrink, M., Martac, E., 2004. Tracer tests for the investigation of heterogeneous porous media and stochastic modelling of flow and transport—a review of some recent developments. J. Hydrology 294 (1), 122–163.
Ren, X., Chen, C., Nagatsu, M., Wang, X., 2011. Carbon nanotubes as adsorbents in environmental pollution management: a review. Chem. Eng. J. 170 (2–3), 395–410.
Schijven, J.F., Hassanizadeh, S.M., 2000. Removal of viruses by soil passage: overview of modeling, processes, and parameters. Crit. Rev. Environ. Sci. Technol. 30 (1), 49–127.
Šimůnek, J., Genuchten, M.T.v., Šejna, M., 2016. Recent developments and applications of the Hydrus computer software packages. Vadose Zone J. 6 (15).
Šimůnek, J., He, C., Pang, L., Bradford, S.A., 2006. Colloid-facilitated solute transport in variably saturated porous media. Vadose Zone J. 5 (3), 1035.
Šimůnek, J., Šejna, M., Genuchten, M.T.v., 2012. The C-Ride module for Hydrus (2D/3D): simulating two-dimensional colloid-facilitated solute transport. In: Variably-saturated Porous Media.
Su, C., Zeng, G.-M., Gong, J.-L., Yang, C.-P., Wan, J., Hu, L., Hua, S.-S., Guo, Y.-Y., 2016. Impact of carbon nanotubes on the mobility of sulfonamide antibiotics in sediments in the Xiangjiang river. RSC Adv. 6 (21), 16941–16951.
Tamtam, F., Mercier, F., Le Bot, B., Eurin, J., Dinh, Q.T., Clément, M., Chevreuil, M., 2008. Occurrence and fate of antibiotics in the seine river in various hydrological conditions. Sci. Total Environ. 393 (1), 84–95.
Tian, Y., Gao, B., Wang, Y., Morales, V.L., Carpena, R.M., Huang, Q., Yang, L., 2012. Deposition and transport of functionalized carbon nanotubes in water-saturated sand columns. J. Hazard. Mater. 213–214, 265–272.
Tong, M., Johnson, W.P., 2007. Colloid population heterogeneity drives hyperexponential deviation from classic filtration theory. Environ. Sci. Technol. 41 (2), 493–499.
Treumann, S., Torkzaban, S., Bradford, S.A., Visalakshan, R.M., Page, D., 2014. An explanation for differences in the process of colloid adsorption in batch and column studies. J. Contam. Hydrology 164, 219–229.
Tufenkji, N., Elimelech, M., 2005. Spatial distributions of cryptosporidium oocysts in porous media: evidence for dual mode deposition. Environ. Sci. Technol. 39 (10), 3620–3629.
Unold, M., Kasteel, R., Groeneweg, J., Vereecken, H., 2009. Transport and transformation of sulfadiazine in soil columns packed with a silty loam and a loamy sand. J. Contam. Hydrology 103 (1–2), 38–47.
Upadhyayula, V.K., Deng, S., Mitchell, M.C., Smith, G.B., 2009. Application of carbon nanotube Technology for removal of contaminants in drinking water: a review. Sci. Total Environ. 408 (1), 1–13.
van de Weerd, H., Leijnse, A., 1997. Assessment of the effect of kinetics on colloid facilitated radionuclide transport in porous media. J. Contam. Hydrology 26 (1), 245–256.
Van Genuchten, M.T., Wagenet, R., 1989. Two-site/two-region models for pesticide transport and degradation: theoretical development and analytical solutions. Soil Sci. Soc. Am. J. 53 (5), 1303–1310.
Wang, D., Paradelo, M., Bradford, S.A., Peijnenburg, W.J., Chu, L., Zhou, D., 2011. Facilitated transport of Cu with hydroxyapatite nanoparticles in saturated sand: effects of solution ionic strength and composition. Water Res. 45 (18), 5905–5915.
Wang, Y., Kim, J.H., Baek, J.B., Miller, G.W., Pennell, K.D., 2012. Transport behavior of functionalized multi-wall carbon nanotubes in water-saturated quartz sand as a function of tube length. Water Res. 46 (14), 4521–4531.
Wehrhan, A., Kasteel, R., Šimůnek, J., Groeneweg, J., Vereecken, H., 2007. Transport of sulfadiazine in soil columns: experiments and modelling approaches. J. Contam. Hydrology 89 (1–2), 107–135.
Woignier, T., Fernandes, P., Jannoyer-Lesueur, M., Soler, A., 2012. Sequestration of chlordecone in the porous structure of an andosol and effects of added organic matter: an alternative to decontamination. Eur. J. Soil Sci. 63 (5), 717–723.
Zarfl, C., 2008. Chemical Fate of Sulfadiazine in Soil: Mechanisms and Modelling Approaches (Shaker).
Zhang, L., Wang, L., Zhang, P., Kan, A.T., Chen, W., Tomson, M.B., 2011. Facilitated transport of 2,2′,5,5′-polychlorinated biphenyl and phenanthrene by fullerene nanoparticles through sandy soil columns. Environ. Sci. Technol. 45 (4), 1341–1348.